Probing R-parity violating supersymmetric effects in the exclusive $b \to c\ell^- \bar{\nu}_\ell$ decays

Ru-Min Wang,[1,*] Jie Zhu,[1,2] Hua-Min Gan,[1] Ying-Ying Fan,[1] Qin Chang,[2] and Yuan-Guo Xu[1,†]

[1] *Institute of Theoretical Physics, Xinyang Normal University, Xinyang, Henan 464000, China*

[2] *Institute of Particle and Nuclear Physics, Henan Normal University, Xinxiang, Henan 453007, China*

(Received 2 March 2016; published 23 May 2016)

Motivated by recent results from the LHCb, *BABAR*, and Belle Collaborations on $B \to D^{(*)}\ell^- \bar{\nu}_\ell$ decays, which significantly deviate from the Standard Model and hint at the possible new physics beyond the Standard Model, we probe the R-parity violating supersymmetric effects in $B_c^- \to \ell^- \bar{\nu}_\ell$ and $B \to D^{(*)}\ell^- \bar{\nu}_\ell$ decays. We find the following: (i) $\mathcal{B}(B_c^- \to e^- \bar{\nu}_e)$ and $\mathcal{B}(B_c^- \to \mu^- \bar{\nu}_\mu)$ are sensitive to the constrained slepton exchange couplings. (ii) The normalized forward-backward asymmetries of $B \to De^- \bar{\nu}_e$ decays have been greatly affected by the constrained slepton exchange couplings, and their signs could be changed. (iii) All relevant observables in the exclusive $b \to c\tau^- \bar{\nu}_\tau$ decays and ratios $\mathcal{R}(D^{(*)})$ are sensitive to the slepton exchange coupling, and $\mathcal{R}(D^*)$ could be enhanced by the constrained slepton exchange coupling to reach each 95% confidence level experimental ranges from *BABAR*, Belle, and LHCb but not the lower limit of the 95% confidence level experimental average. Our results in this work could be used to probe R-parity violating effects and will correlate with searches for direct supersymmetric signals at the running LHCb and the forthcoming Belle-II.

DOI: 10.1103/PhysRevD.93.094023

I. INTRODUCTION

The semileptonic decays $B \to D^{(*)}\ell^- \bar{\nu}_\ell$ are very important processes in testing the Stand Model (SM) and in searching for the new physics (NP) beyond the SM, for example, the extraction of the Cabbibo-Kobayashi-Maskawa matrix element $|V_{cb}|$. The semileptonic decays $B \to D^{(*)}\ell^- \bar{\nu}_\ell$ have been measured by the CLEO [1], Belle [2,3], *BABAR* [4–7], and LHCb [8] Collaborations. For ratios $\mathcal{R}(D^{(*)}) \equiv \frac{\mathcal{B}(B\to D^{(*)}\tau^- \bar{\nu}_\tau)}{\mathcal{B}(B\to D^{(*)}\ell'^- \bar{\nu}_{\ell'})}$ with $\ell' = e$ or μ, the experimental averages from the Heavy Flavor Averaging Group [9] are

$$\mathcal{R}(D)^{\mathrm{Exp}} = 0.391 \pm 0.050,$$
$$\mathcal{R}(D^*)^{\mathrm{Exp}} = 0.322 \pm 0.021. \quad (1)$$

The SM predictions [10,11] are

$$\mathcal{R}(D)^{\mathrm{SM}} = 0.297 \pm 0.017,$$
$$\mathcal{R}(D^*)^{\mathrm{SM}} = 0.252 \pm 0.003. \quad (2)$$

The experimental measurements of $\mathcal{R}(D)$ and $\mathcal{R}(D^*)$ differ from their SM predictions by 1.7σ and 3.0σ deviations, respectively, and these hint at the possible NP beyond the SM.

The exclusive $b \to c\ell^- \bar{\nu}_\ell$ decays have been studied extensively in the framework of the SM and various NP models, see Refs. [12–39]. Supersymmetry (SUSY) is one of the most widely discussed options of NP, in both its R-parity conserving and R-parity violating (RPV) incarnations [40,41]. In the SUSY with R-parity conservation, the charged Higgs contribution could enter at tree level, similar to the exclusive $b \to u\ell^- \bar{\nu}_\ell$ studied in Ref. [42]. The charged Higgs contributions can slightly reduce $\mathcal{B}(B \to D^{(*)}\tau^- \bar{\nu}_\tau)$, but the effects of the charged Higgs will not significantly affect the light leptonic decays. Therefore, the charged Higgs effects could let $\mathcal{R}(D^{(*)})$ deviate more from their experimental data. In fact, none of the 2HDMs with natural flavor conservation can explain the excess in $\mathcal{R}(D^*)$ [43]. In the SUSY with R-parity violation, B meson decays have been extensively investigated, see Refs. [44–52]. In this paper, we explore the RPV effects in the leptonic and semileptonic exclusive $b \to c\ell^- \bar{\nu}_\ell$ decays. We constrain relevant RPV parameter spaces from present experimental measurements and analyze their contributions to the branching ratios, differential branching ratios, normalized forward-backward (FB) asymmetries of the charged leptons, and ratios of the branching ratios of relevant semileptonic B decays.

The paper is organized as follows. In Sec. II, we briefly review the theoretical results of the exclusive $b \to c\ell^- \bar{\nu}_\ell$ decays in the RPV SUSY model. In Sec. III, using the constrained parameter spaces from relevant experimental measurements, we make a detailed classification research on the RPV effects on the quantities which have not been measured or not been well measured yet. Our conclusions are given in Sec. IV.

*ruminwang@sina.com
†yuanguoxv@163.com

II. THE EXCLUSIVE $b \to c\ell^- \bar{\nu}_\ell$ DECAYS IN THE SUSY WITHOUT R-PARITY

Regarding the RPV SUSY model, similar processes $b \to u\ell^- \bar{\nu}_\ell$ have been studied in Ref. [42], so we only give the final expressions in this section.

The branching ratio for the pure leptonic decays $B_c^- \to \ell_m^- \bar{\nu}_{\ell_n}$ can be written as [42]

$$\mathcal{B}(B_c^- \to \ell_m^- \bar{\nu}_{\ell_n}) = \left| \frac{G_F}{\sqrt{2}} V_{cb} - \sum\nolimits_i \frac{\lambda'_{n3i} \tilde{\lambda}'^*_{m2i}}{8 m^2_{\tilde{d}_{iR}}} + \sum\nolimits_i \frac{\lambda_{inm} \tilde{\lambda}'^*_{i23}}{4 m^2_{\tilde{\ell}_{iL}}} \frac{\mu_{B_c}}{m_\ell} \right|^2 \frac{\tau_{B_c}}{4\pi} f^2_{B_c} m_{B_c} m^2_\ell \left[1 - \frac{m^2_\ell}{m^2_{B_c}}\right]^2, \tag{3}$$

where $\mu_{B_c} \equiv m^2_{B_c}/(\bar{m}_b + \bar{m}_c)$.

The differential branching ratios for the semileptonic decays $B \to D\ell_m^- \bar{\nu}_{\ell_n}$ could be written as [42]

$$\frac{d\mathcal{B}(B \to D\ell^- \bar{\nu}_{\ell_n})}{ds\, d\cos\theta} = \frac{\tau_B \sqrt{\lambda_D}}{2^7 \pi^3 m_B^3} \left(1 - \frac{m^2_{\ell_m}}{s}\right)^2 [N_0^D + N_1^D \cos\theta + N_2^D \cos^2\theta], \tag{4}$$

with

$$\begin{aligned} N_0^D = {} & \left| \frac{G_F}{\sqrt{2}} V_{cb} - \sum\nolimits_i \frac{\lambda'_{n3i} \tilde{\lambda}'^*_{m2i}}{8 m^2_{\tilde{d}_{iR}}} \right|^2 [f_+^D(s)]^2 \lambda_D \\ & + \left| \frac{G_F}{\sqrt{2}} V_{cb} - \sum_i \frac{\lambda'_{n3i} \tilde{\lambda}'^*_{m2i}}{8 m^2_{\tilde{d}_{iR}}} + \sum\nolimits_i \frac{\lambda_{inm} \tilde{\lambda}'^*_{i23}}{4 m^2_{\tilde{\ell}_{iL}}} \frac{s}{m_{\ell_m}(\bar{m}_b - \bar{m}_c)} \right|^2 m^2_{\ell_m} [f_0^D(s)]^2 \frac{(m_B^2 - m_D^2)^2}{s}, \end{aligned} \tag{5}$$

$$\begin{aligned} N_1^D = {} & \left\{ \left| \frac{G_F}{\sqrt{2}} V_{cb} - \sum\nolimits_i \frac{\lambda'_{n3i} \tilde{\lambda}'^*_{m2i}}{8 m^2_{\tilde{d}_{iR}}} \right|^2 + \mathrm{Re}\left[\left(\frac{G_F}{\sqrt{2}} V_{cb} - \sum\nolimits_i \frac{\lambda'_{n3i} \tilde{\lambda}'^*_{m2i}}{8 m^2_{\tilde{d}_{iR}}} \right)^\dagger \right.\right. \\ & \left.\left. \times \sum_i \frac{\lambda_{inm} \tilde{\lambda}'^*_{i23}}{4 m^2_{\tilde{\ell}_{iL}}} \frac{s}{m_{\ell_m}(\bar{m}_b - \bar{m}_c)} \right] \right\} 2 m^2_{\ell_m} f_0^D(s) f_+^D(s) \sqrt{\lambda_D} \frac{(m_B^2 - m_D^2)}{s}, \end{aligned} \tag{6}$$

$$N_2^D = -\left| \frac{G_F}{\sqrt{2}} V_{cb} - \sum\nolimits_i \frac{\lambda'_{n3i} \tilde{\lambda}'^*{}_{m2i}}{8 m^2_{\tilde{d}_{iR}}} \right|^2 [f_+^D(s)]^2 \lambda_D \left(1 - \frac{m^2_{\ell_m}}{s}\right). \tag{7}$$

The differential branching ratios for the semileptonic decays $B \to D^* \ell_m^- \bar{\nu}_{\ell_n}$ could be written as [42]

$$\frac{d\mathcal{B}(B \to D^* \ell_m^- \bar{\nu}_{\ell_n})}{ds\, d\cos\theta} = \frac{\tau_B \sqrt{\lambda_D^*}}{2^7 \pi^3 m_B^3} \left(1 - \frac{m^2_{\ell_m}}{s}\right)^2 [N_0^{D^*} + N_1^{D^*} \cos\theta + N_2^{D^*} \cos^2\theta], \tag{8}$$

with

$$\begin{aligned} N_0^{D^*} = {} & \left| \frac{G_F}{\sqrt{2}} V_{cb} - \sum\nolimits_i \frac{\lambda'_{n3i} \tilde{\lambda}'^*_{m2i}}{8 m^2_{\tilde{d}_{iR}}} \right|^2 \left\{ [A_1^{D^*}(s)]^2 \left(\frac{\lambda_{D^*}}{4 m^2_{D^*}} + (m^2_{\ell_m} + 2s) \right) (m_B + m_{D^*})^2 \right. \\ & \left. + [A_2^{D^*}(s)]^2 \frac{\lambda^2_{D^*}}{4 m_V^2 (m_B + m_{D^*})^2} + [V^{D^*}(s)]^2 \frac{\lambda_{D^*}}{(m_B + m_{D^*})^2} (m^2_{\ell_m} + s) - A_1^{D^*}(s) A_2^{D^*}(s) \frac{\lambda_{D^*}}{2 m^2_{D^*}} (m_B^2 - s - m^2_{D^*}) \right\} \\ & + \left| \frac{G_F}{\sqrt{2}} V_{cb} - \sum\nolimits_i \frac{\lambda'_{n3i} \tilde{\lambda}'^*_{m2i}}{8 m^2_{\tilde{d}_{iR}}} + \sum\nolimits_i \frac{\lambda_{inm} \tilde{\lambda}'^*_{i23}}{4 m^2_{\tilde{\ell}_{iL}}} \frac{s}{m_{\ell_m}(\bar{m}_b + \bar{m}_c)} \right|^2 [A_0^{D^*}(s)]^2 \frac{m^2_{\ell_m}}{s} \lambda_{D^*}, \end{aligned} \tag{9}$$

$$N_1^{D^*} = \left\{ \left| \frac{G_F}{\sqrt{2}} V_{cb} - \sum\nolimits_i \frac{\lambda'_{n3i}\tilde{\lambda}'^*_{m2i}}{8m^2_{\tilde{d}_{iR}}} \right|^2 + \mathrm{Re}\left[\left(\frac{G_F}{\sqrt{2}} V_{cb} - \sum\nolimits_i \frac{\lambda'_{n3i}\tilde{\lambda}'^*_{m2i}}{8m^2_{\tilde{d}_{iR}}} \right)^\dagger \sum_i \frac{\lambda_{inm}\tilde{\lambda}'^*_{i23}}{4m^2_{\tilde{\ell}_{iL}}} \frac{s}{m_{\ell_m}(\bar{m}_b + \bar{m}_c)} \right] \right\}$$
$$\times \left[A_0^{D^*}(s) A_1^{D^*}(s) \frac{m^2_{\ell_m}(m_B + m_{D^*})(m_B^2 - m^2_{D^*} - s)\sqrt{\lambda_{D^*}}}{s m_{D^*}} - A_0^{D^*}(s) A_2^{D^*}(s) \frac{m^2_{\ell_m}\lambda^{3/2}_{D^*}}{s m_{D^*}(m_B + m_{D^*})} \right]$$
$$+ \left| \frac{G_F}{\sqrt{2}} V_{cb} - \sum\nolimits_i \frac{\lambda'_{n3i}\tilde{\lambda}'^*_{m2i}}{8m^2_{\tilde{d}_{iR}}} \right|^2 A_1^{D^*}(s) V^{D^*}(s) 4s\sqrt{\lambda_{D^*}}, \tag{10}$$

$$N_2^{D^*} = -\left| \frac{G_F}{\sqrt{2}} V_{cb} - \sum\nolimits_i \frac{\lambda'_{n3i}\tilde{\lambda}'^*_{m2i}}{8m^2_{\tilde{d}_{iR}}} \right|^2 \left(1 - \frac{m^2_{\ell_m}}{s}\right) \lambda_{D^*} \left\{ [A_1^{D^*}(s)]^2 \frac{(m_B + m_{D^*})^2}{4m^2_{D^*}} + [V^{D^*}(s)]^2 \frac{s}{(m_B + m_{D^*})^2} \right.$$
$$\left. + [A_2^{D^*}(s)]^2 \frac{\lambda_{D^*}}{4m^2_{D^*}(m_B + m_{D^*})^2} - A_1^{D^*}(s) A_2^{D^*}(s) \frac{m_B^2 - m^2_{D^*} - s}{2m^2_{D^*}} \right\}, \tag{11}$$

where $s = q^2 = (p_B - p_{D^{(*)}})^2$, the kinematic factor $\lambda_{D^{(*)}} = m_B^4 + m^4_{D^{(*)}} + s^2 - 2m_B^2 m^2_{D^{(*)}} - 2m_B^2 s - 2m^2_{D^{(*)}} s$, and θ is the angle between the momentum of B meson and the charged lepton in the c.m. system of $\ell - \nu$.

The normalized forward-backward asymmetries of the charged lepton $\bar{\mathcal{A}}^{D^{(*)}}_{\mathrm{FB}}$ are given as [42]

$$\bar{\mathcal{A}}_{\mathrm{FB}}(B \to D^{(*)}\ell^-_m\bar{\nu}_{\ell_n}) = \frac{N_1^{D^{(*)}}}{2N_0^{D^{(*)}} + 2/3N_2^{D^{(*)}}}. \tag{12}$$

From the above expressions, we can see that, unlike the contributions of the squark exchange couplings $\lambda'_{n3i}\tilde{\lambda}'^*_{m2i}$ and the SM contributions, the slepton exchange couplings $\lambda_{inm}\tilde{\lambda}'^*_{i23}$ will not be suppressed by s and helicity.

III. NUMERICAL RESULTS AND DISCUSSIONS

In the numerical calculations, the main theoretical input parameters are the transition form factors, decay constant of B_c^- meson, masses, mean lives, CKM matrix element, etc. For the transition form factors, the traditional approaches to calculate the relevant transition form factors are the heavy quark effective theory [10,28], lattice QCD techniques [15,16], and pQCD factorization approach with and without lattice QCD input [31–33]. We use the form factors based on the heavy quark effective theory [10,28]. The decay constant of B_c^- meson is taken from Ref. [53], and the rest of the theoretical input parameters are taken from the Particle Data Group (PDG) [54]. Notice that we assume the masses of the corresponding slepton are 500 GeV. For other values of the slepton masses, the bounds on the couplings in this paper can be easily obtained by scaling them by factor $\tilde{f}^2 \equiv (\frac{m_{\tilde{\ell}}}{500\ \mathrm{GeV}})^2$.

In our calculation, we consider only one NP coupling at one time and keep its interference with the SM amplitude to study the RPV SUSY effects. To be conservative, the input parameters and the experimental bounds except for $\mathcal{B}(B \to D^*\tau^-\bar{\nu}_\tau)$ and $\mathcal{R}(D^*)$ at a 95% confidence level (C.L.) are used to constrain parameter spaces of the relevant new couplings. Note that we do not impose the experimental bounds from $\mathcal{B}(B \to D^*\tau^-\bar{\nu}_\tau)$ and $\mathcal{R}(D^*)$ since their experimental measurements obviously deviate from their SM predictions. We leave them as predictions of the restricted parameter spaces of the RPV couplings and then compare them with the experimental results.

Due to the strong helicity suppression, the squark exchange couplings have no very obvious effects on the differential branching ratios and the normalized FB asymmetries of the semileptonic exclusive $b \to c\ell^-_m\bar{\nu}_{\ell_n}$ decays. So, we only focus on the slepton exchange couplings in our following discussions. For the slepton exchange couplings, $\lambda_{i11}\tilde{\lambda}'^*_{i23}$ and $\lambda_{i22}\tilde{\lambda}'^*_{i23}$, which contribute to both $b \to c\ell'^-_m\bar{\nu}_{\ell'_n}$ and $b \to s\ell'^+_m\ell'^-_n$ transitions, the stronger constraints are from the exclusive $b \to s\ell'^+_m\ell'^-_n$ decays [46,49]; nevertheless, the RPV weak phases of the two slepton exchange couplings are not obviously constrained by current experimental measurements.

A. Exclusive $b \to ce^-\bar{\nu}_e$ decays

First, we focus on slepton exchange couplings $\lambda_{i11}\tilde{\lambda}'^*_{i23}$ contributing to five decay modes, $B_c^- \to e^-\bar{\nu}_e$, $B_u^- \to D_u^0 e^-\bar{\nu}_e$, $B_u^- \to D_u^{*0} e^-\bar{\nu}_e$, $B_d^0 \to D_d^+ e^-\bar{\nu}_e$, and $B_d^0 \to D_d^{*+} e^-\bar{\nu}_e$ decays. The branching ratios of four semileptonic processes have been accurately measured by CLEO [1], Belle [2], and *BABAR* [5,6] Collaborations. The 95% C.L. ranges of the experimental average values from the PDG [54] are listed in the second column of Table I. The SM predictions at the 95% C.L. are presented in the third column of Table I.

TABLE I. Branching ratios of the exclusive $b \to ce^-\bar{\nu}_e$ decays (in units of 10^{-2}) except for $\mathcal{B}(B_c^- \to e^-\bar{\nu}_e)$ (in units of 10^{-9}). The experimental ranges and the SM predictions at the 95% C.L. are listed in the second and third columns, respectively. In the last column, "SUSY/$\lambda_{i11}\tilde{\lambda}'^*_{i23}$" denotes the SUSY predictions considering the constrained $\lambda_{i11}\tilde{\lambda}'^*_{i23}$ couplings. Similar terms are used in Tables II and III.

Observable	Exp. data	SM predictions	SUSY/$\lambda_{i11}\tilde{\lambda}'^*_{i23}$
$\mathcal{B}(B_c^- \to e^-\bar{\nu}_e)$	$\cdots$	[1.39, 2.72]	[1.49×10^{-2}, 1068]
$\mathcal{B}(B_u^- \to D_u^0 e^-\bar{\nu}_e)$	[2.05, 2.49]	[1.81, 2.91]	[2.10, 2.49]
$\mathcal{B}(B_u^- \to D_u^{*0} e^-\bar{\nu}_e)$	[5.32, 6.06]	[4.78, 5.81]	[5.34, 5.61]
$\mathcal{B}(B_d^0 \to D_d^+ e^-\bar{\nu}_e)$	[1.95, 2.43]	[1.68, 2.69]	[1.96, 2.33]
$\mathcal{B}(B_d^0 \to D_d^{*+} e^-\bar{\nu}_e)$	[4.71, 5.15]	[4.44, 5.38]	[4.89, 5.15]

Using the experimental bounds of relevant exclusive $b \to c\ell^-\bar{\nu}_\ell$ decays at the 95% C.L.,[1] we obtain the slepton exchange couplings $|\lambda_{i11}\tilde{\lambda}'^*_{i23}| \leq 0.22$. At present, the strongest bounds on the slepton exchange couplings come from the exclusive $b \to se^+e^-$ decays, $|\lambda_{i11}\tilde{\lambda}'^*_{i23}| \leq 5.75 \times 10^{-4}$ with 500 GeV slepton masses [46], which will be used in our numerical results. In addition, the experimental bounds at the 95% C.L. listed in the second column of Table I are also considered to further constrain the slepton exchange couplings. Our numerical results of the relevant branching ratios, which consider the constrained slepton exchange couplings, are listed in the last column of Table I, and we can see that the constrained slepton exchange coupling has significant effects on $\mathcal{B}(B_c^- \to e^-\bar{\nu}_e)$, which could be suppressed 2 orders or enhanced 3 orders by the constrained slepton exchange couplings. Nevertheless, the constrained slepton exchange couplings have no significant effects on the branching ratios of relevant semileptonic decays.

For $B_u^- \to D_u^{(*)0}e^-\bar{\nu}_e$ and $B_d^0 \to D_d^{(*)+}e^-\bar{\nu}_e$ decays, since the $SU(2)$ flavor symmetry implies $\mathcal{M}(B_u^- \to D_u^{(*)0}e^-\bar{\nu}_e) \simeq \mathcal{M}(B_d^0 \to D_d^{(*)+}e^-\bar{\nu}_e)$, the slepton exchange RPV contributions to $B_u^- \to D_u^{(*)0}e^-\bar{\nu}_e$ and $B_d^0 \to D_d^{(*)+}e^-\bar{\nu}_e$ are very similar to each other. So, we take $B_u^- \to D_u^{(*)0}e^-\bar{\nu}_e$ decays as examples. This is similar in the exclusive $b \to c\mu^-\bar{\nu}_\mu$ and $b \to c\tau^-\bar{\nu}_\tau$ decays.

Figure 1 shows the constrained RPV effects of $\lambda_{i11}\tilde{\lambda}'^*_{i23}$ on $\mathcal{B}(B_c^- \to e^-\bar{\nu}_e)$, $d\mathcal{B}(B_u^- \to D^{(*)0}e^-\bar{\nu}_e)/ds$ and $\bar{\mathcal{A}}_{\mathrm{FB}}(B_u^- \to D^{(*)0}e^-\bar{\nu}_e)$. The SM results are also displayed for comparing. Comparing the RPV SUSY predictions to the SM ones, we have the following remarks:

(i) As shown in Figs. 1(a) and 1(b), $\mathcal{B}(B_c^- \to e^-\bar{\nu}_e)$ is very sensitive to both the moduli and weak phases of the $\lambda_{i11}\tilde{\lambda}'^*_{i23}$ couplings, and this is because the slepton exchange coupling effects on $\mathcal{B}(B_c^- \to e^-\bar{\nu}_e)$ is increased by m_B/m_e.

(ii) As displayed in Figs. 1(c) and 1(d), there are no obvious RPV effects on $d\mathcal{B}(B_u^- \to D_u^{(*)0}e^-\bar{\nu}_e)$ since the present accurate experimental measurements of $\mathcal{B}(B_u^- \to D_u^{*0}e^-\bar{\nu}_e, B_d^0 \to D_d^{*+}e^-\bar{\nu}_e)$ give very strongly constraints on the slepton exchange couplings. For the same reason, the branching ratios of relevant semileptonic decays are not sensitive to both the moduli and weak phases of the $\lambda_{i11}\tilde{\lambda}'^*_{i23}$ couplings, so we do not display them in Fig. 1.

(iii) Figure 1(e) shows us that the constrained $\lambda_{i11}\tilde{\lambda}'^*_{i23}$ couplings provide quite obvious effects on $\bar{\mathcal{A}}_{\mathrm{FB}}(B_u^- \to D_u^0 e^-\bar{\nu}_e)$. Its sign could be changed; nevertheless, this quantity is tiny. Figure 1(f) shows that there is no obvious RPV effect on $\bar{\mathcal{A}}_{\mathrm{FB}}(B_u^- \to D_u^{*0}e^-\bar{\nu}_e)$.

B. Exclusive $b \to c\mu^-\bar{\nu}_\mu$ decays

Now, we pay attention to the contributions of the slepton exchange couplings $\lambda_{i22}\tilde{\lambda}'^*_{i23}$ to $B_c^- \to \mu^-\bar{\nu}_\mu$, $B_u^- \to D_u^0\mu^-\bar{\nu}_\mu$, $B_u^- \to D_u^{*0}\mu^-\bar{\nu}_\mu$, $B_d^0 \to D_d^+\mu^-\bar{\nu}_\mu$, and $B_d^0 \to D_d^{*+}\mu^-\bar{\nu}_\mu$ decays. The four semileptonic decay branching ratios have been accurately measured by CLEO [1], Belle [2], and *BABAR* [5,6] Collaborations. The experimental average values and the SM predictions at the 95% C.L. are listed in the second and third columns of Table II, respectively.

We get the slepton exchange couplings $|\lambda_{i22}\tilde{\lambda}'^*_{i23}| < 0.24$ from the exclusive $b \to c\ell^-\bar{\nu}_\ell$ decays, which are a lot weaker than ones from the exclusive $b \to s\mu^+\mu^-$ decays, $|\lambda_{i22}\tilde{\lambda}'^*_{i23}| < 2.0 \times 10^{-4}$ with 500 GeV slepton masses [49]. Taking the strongest bounds from the exclusive $b \to s\mu^+\mu^-$ decays and further considering the experimental bounds from the exclusive $b \to c\ell^-\bar{\nu}_\ell$ decays, we predict the constrained slepton exchange effects in the exclusive

[1] In general, we should use all present experimental bounds of the exclusive $b \to ce^-\nu_e$ decay, i.e., $\mathcal{B}(B \to D^{(*)}e^-\bar{\nu}_e)$, to constrain parameter spaces of the relevant new couplings for the exclusive $b \to ce^-\nu_e$ decays. In addition, the experimental bound of $\mathcal{R}(D) = \mathcal{B}(B \to D\tau^-\nu)/\mathcal{B}(B \to De^-\nu)$ is also considered to constrain parameter spaces for the exclusive $b \to ce^-\nu_e$ decays. To obtain the best constrained $\mathcal{R}(D)$, the experimental bound constrained on $\mathcal{B}(B \to D\tau^-\nu)$, $\mathcal{R}'(D) = \mathcal{B}(B \to D\tau^-\nu)/\mathcal{B}(B \to D\mu^-\nu)$ and $\mathcal{B}(B \to D\mu^-\nu)$ must be considered, too. Therefore, we use all present experimental bounds of relevant exclusive $b \to c\ell\nu$ decays except for $\mathcal{B}(B \to D^*\tau^-\bar{\nu}_\tau)$ and $\mathcal{R}(D^*)$. This is similar in exclusive $b \to c\mu^-\bar{\nu}_\mu$ and $b \to c\tau^-\bar{\nu}_\tau$ decays.

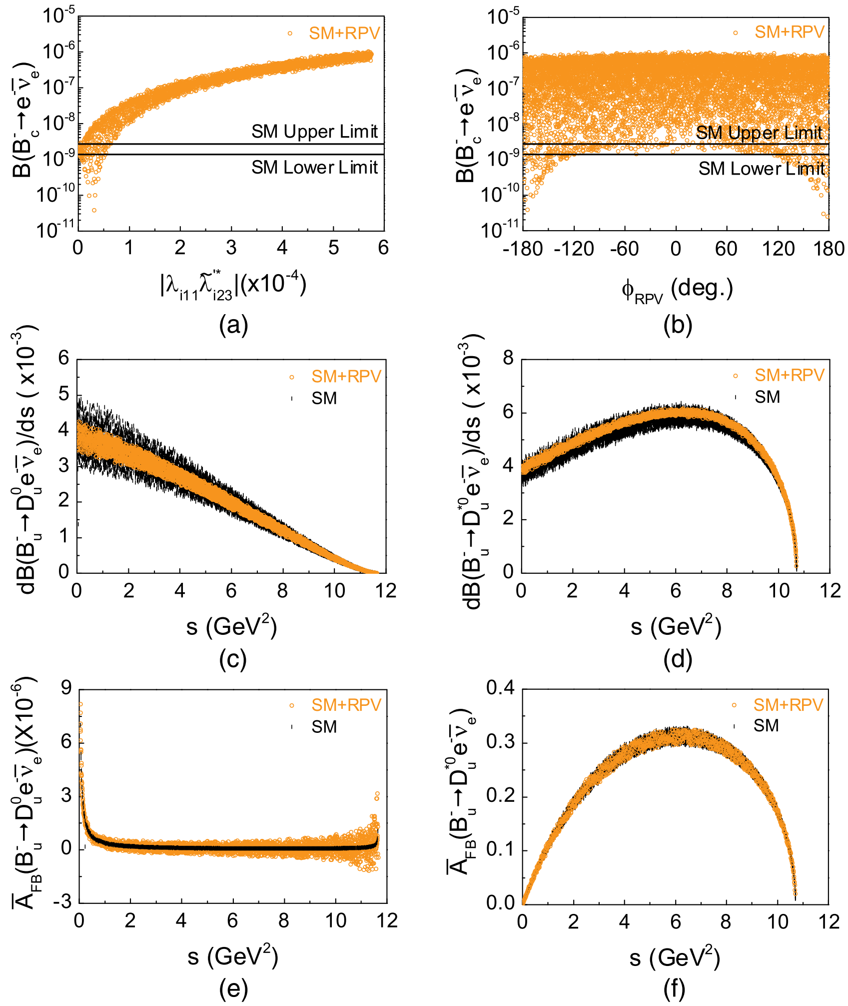

FIG. 1. Constrained slepton exchange coupling effects in the exclusive $b \to c e^- \bar{\nu}_e$ decays.

$b \to c\mu^- \bar{\nu}_\mu$ decays, which are given in the last column of Table II and displayed in Fig. 2. From Table II and Fig. 2, we make the following points:

(i) As displayed in Figs. 2(a) and 2(b), $\mathcal{B}(B_c^- \to \mu^- \bar{\nu}_\mu)$ has some sensitivities to both modulus and weak phases of the $\lambda_{i22}\tilde{\lambda}'^*_{i23}$ couplings, and it has maximum at $\phi_{\mathrm{RPV}} \in [-60°, 60°]$.

(ii) Figure 2(c) and 2(d) shows that the constrained slepton exchange couplings have no obvious contribution to $d\mathcal{B}(B_u^- \to D_u^{(*)0}\mu^-\bar{\nu}_\mu)/ds$, and they are strongly constrained by present experimental data.

(iii) As displayed in Figs. 2(e) and 2(f), the constrained slepton exchange couplings also have no obvious contribution to $\bar{\mathcal{A}}_{\mathrm{FB}}(B_u^- \to D_u^{(*)0}\mu^-\bar{\nu}_\mu)$ at all s ranges. Note that the slepton exchange coupling effects on $\bar{\mathcal{A}}_{\mathrm{FB}}(B_u^- \to D_u^0\mu^-\bar{\nu}_\mu)$ are very different from the ones on $\bar{\mathcal{A}}_{\mathrm{FB}}(B_u^- \to D_u^0 e^-\bar{\nu}_e)$ displayed in Figs. 1(e) and 1(f) since the bounds on $|\lambda_{i22}\tilde{\lambda}'^*_{i23}|$ are about 3 times smaller than ones on $|\lambda_{i11}\tilde{\lambda}'^*_{i23}|$ (the same order of magnitude), and $\bar{\mathcal{A}}_{\mathrm{FB}}(B_u^- \to D_u^0\mu^-\bar{\nu}_\mu)$ is 1000 times larger than $\bar{\mathcal{A}}_{\mathrm{FB}}(B_u^- \to D_u^0 e^-\bar{\nu}_e)$.

TABLE II. Branching ratios of the exclusive $b \to c\mu^-\bar{\nu}_\mu$ decays (in units of 10^{-2}) except for $\mathcal{B}(B_c^- \to \mu^-\bar{\nu}_\mu)$ (in units of 10^{-4}).

Observable	Exp. data	SM predictions	SUSY/$\lambda^*_{i22}\tilde{\lambda}'^*_{i23}$
$\mathcal{B}(B_c^- \to \mu^-\bar{\nu}_\mu)$	…	[0.59, 1.16]	[0.51, 1.17]
$\mathcal{B}(B_u^- \to D_u^0\mu^-\bar{\nu}_\mu)$	[2.05, 2.49]	[1.81, 2.89]	[2.09, 2.48]
$\mathcal{B}(B_u^- \to D_u^{*0}\mu^-\bar{\nu}_\mu)$	[5.32, 6.06]	[4.76, 5.77]	[5.32, 5.59]
$\mathcal{B}(B_d^0 \to D_d^+\mu^-\bar{\nu}_\mu)$	[1.95, 2.43]	[1.68, 2.67]	[1.96, 2.32]
$\mathcal{B}(B_d^0 \to D_d^{*+}\mu^-\bar{\nu}_\mu)$	[4.71, 5.15]	[4.42, 5.35]	[4.87, 5.13]

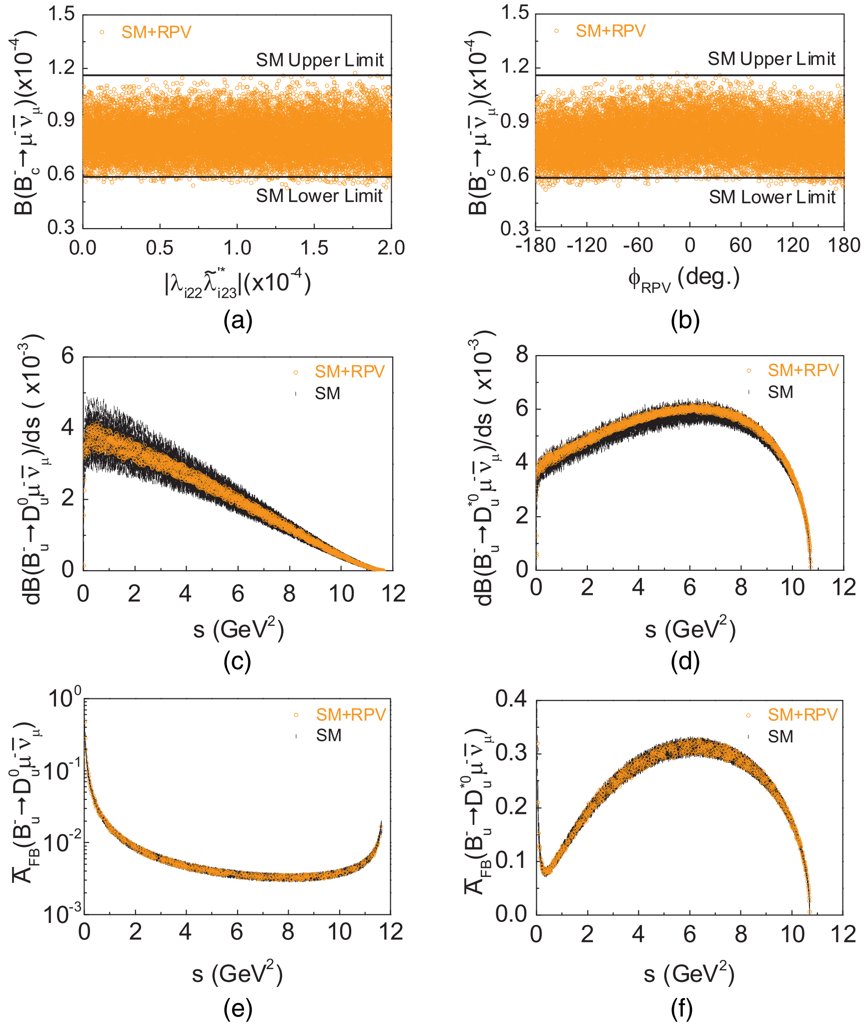

FIG. 2. Constrained slepton exchange coupling effects in the exclusive $b \to c\mu^- \bar{\nu}_\mu$ decays.

C. Exclusive $b \to c\tau^- \bar{\nu}_\tau$ decays

In this subsection, we concentrate on the contributions of the slepton exchange couplings $\lambda_{i33}\tilde{\lambda}'^{*}_{i23}$ in $B_c^- \to \tau^- \bar{\nu}_\tau$, $B_u^- \to D_u^0 \tau^- \bar{\nu}_\tau$, $B_u^- \to D_u^{*0} \tau^- \bar{\nu}_\tau$, $B_d^0 \to D_d^+ \tau^- \bar{\nu}_\tau$, and $B_d^0 \to D_d^{*+} \tau^- \bar{\nu}_\tau$ decays. The precise measurements of these semileptonic branching ratios have been reported by *BABAR*, Belle, and LHCb [3,4,7,8] Collaborations. The 95% C.L. experimental ranges of the average data from PDG [54] and the 95% C.L. SM predictions are listed in the second and the third columns of Table III, respectively.

Figure 3 displays the allowed parameter spaces of the couplings $\lambda_{i33}\tilde{\lambda}'^{*}_{i23}$ from the 95% C.L. experimental bounds of the exclusive $b \to c\ell^- \bar{\nu}_\ell$ decays. Both the moduli and the weak phases of $\lambda_{i33}\tilde{\lambda}'^{*}_{i23}$ are obviously constrained by current experimental measurement. The bounds on $\lambda_{i33}\tilde{\lambda}'^{*}_{i23}$ are obtained for the first time.

TABLE III. Branching ratios of the exclusive $b \to c\tau^- \bar{\nu}_\tau$ decays (in units of 10^{-2}).

Observable	Exp. data	SM predictions	SUSY/$\lambda_{i33}\tilde{\lambda}'^{*}_{i23}$
$\mathcal{B}(B_c^- \to \tau^- \bar{\nu}_\tau)$	$\cdots$	[1.42, 2.78]	[0.87, 100]
$\mathcal{B}(B_u^- \to D_u^0 \tau^- \bar{\nu}_\tau)$	[0.28, 1.26]	[0.52, 0.90]	[0.64, 1.20]
$\mathcal{B}(B_u^- \to D_u^{*0} \tau^- \bar{\nu}_\tau)$	[1.49, 2.27]	[1.21, 1.47]	[1.21, 1.53]
$\mathcal{B}(B_d^0 \to D_d^+ \tau^- \bar{\nu}_\tau)$	[0.60, 1.46]	[0.48, 0.84]	[0.60, 1.12]
$\mathcal{B}(B_d^0 \to D_d^{*+} \tau^- \bar{\nu}_\tau)$	[1.41, 2.27]	[1.12, 1.36]	[1.12, 1.41]

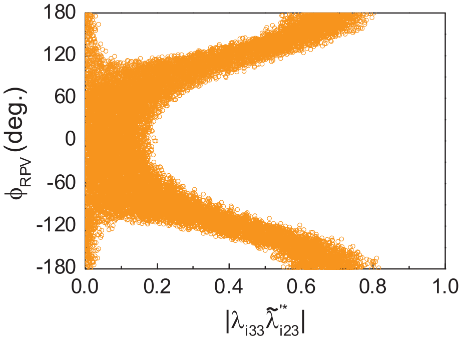

FIG. 3. Allowed parameter spaces of $\lambda_{i33}\tilde{\lambda}'^{*}_{i23}$ from the 95% C.L. experimental bounds of the exclusive $b \to c\ell^-\bar{\nu}_\ell$ decays.

Now, we discuss the constrained $\lambda_{i33}\tilde{\lambda}'^{*}_{i23}$ effects in the exclusive $b \to c\tau^-\bar{\nu}_\tau$ decays. Our numerical predictions are given in the last column of Table III. Figure 4 shows the sensitivities of the branching ratios to both the moduli and weak phases of $\lambda_{i33}\tilde{\lambda}'^{*}_{i23}$, and Fig. 6 shows the constrained slepton exchange effects on the differential branching ratios and the normalized FB asymmetries of $B_u^- \to D_u^{(*)0}\tau^-\bar{\nu}_\tau$ decays.

As displayed in Figs. 4(a) and 4(b), $\mathcal{B}(B_c^- \to \tau^-\bar{\nu}_\tau)$ is very sensitive to both the moduli and weak phases of $\lambda_{i33}\tilde{\lambda}'^{*}_{i23}$, so the future experimental measurements on $\mathcal{B}(B_c^- \to \tau^-\bar{\nu}_\tau)$ will give a quite strong bound on $\lambda_{i33}\tilde{\lambda}'^{*}_{i23}$. As displayed in Figs. 4(c) and 4(d), $\mathcal{B}(B_u^- \to D_u^0\tau^-\bar{\nu}_\tau)$ is sensitive to $|\lambda_{i33}\tilde{\lambda}'^{*}_{i23}|$ but not sensitive to their weak phases. As shown in Fig. 3, we get quite a strong constraint on both the modulus and weak phase of $\lambda_{i33}\tilde{\lambda}'^{*}_{i23}$ from the experimental bounds of $\mathcal{B}(B \to D\tau^-\bar{\nu}_\tau)$ and $\mathcal{R}(D)$. Nevertheless, from Figs. 4(c) and 4(d), we can see that the experimental bound of $\mathcal{B}(B \to D\tau^-\bar{\nu}_\tau)$ does not give any effective constraint to both the modulus and weak phase of $\lambda_{i33}\tilde{\lambda}'^{*}_{i23}$, therefore, the present experimental measurement of $\mathcal{R}(D)$ gives quite strong bounds on $\lambda_{i33}\tilde{\lambda}'^{*}_{i23}$ and $\mathcal{B}(B_u^- \to D_u^0\tau^-\bar{\nu}_\tau)$. As displayed in Figs. 4(e) and 4(f), $\mathcal{B}(B_u^- \to D_u^{*0}\tau^-\bar{\nu}_\tau)$ is very sensitive to both the moduli and weak phases of $\lambda_{i33}\tilde{\lambda}'^{*}_{i23}$ couplings. In fact, $|\lambda_{i33}\tilde{\lambda}'^{*}_{i23}|$ and its

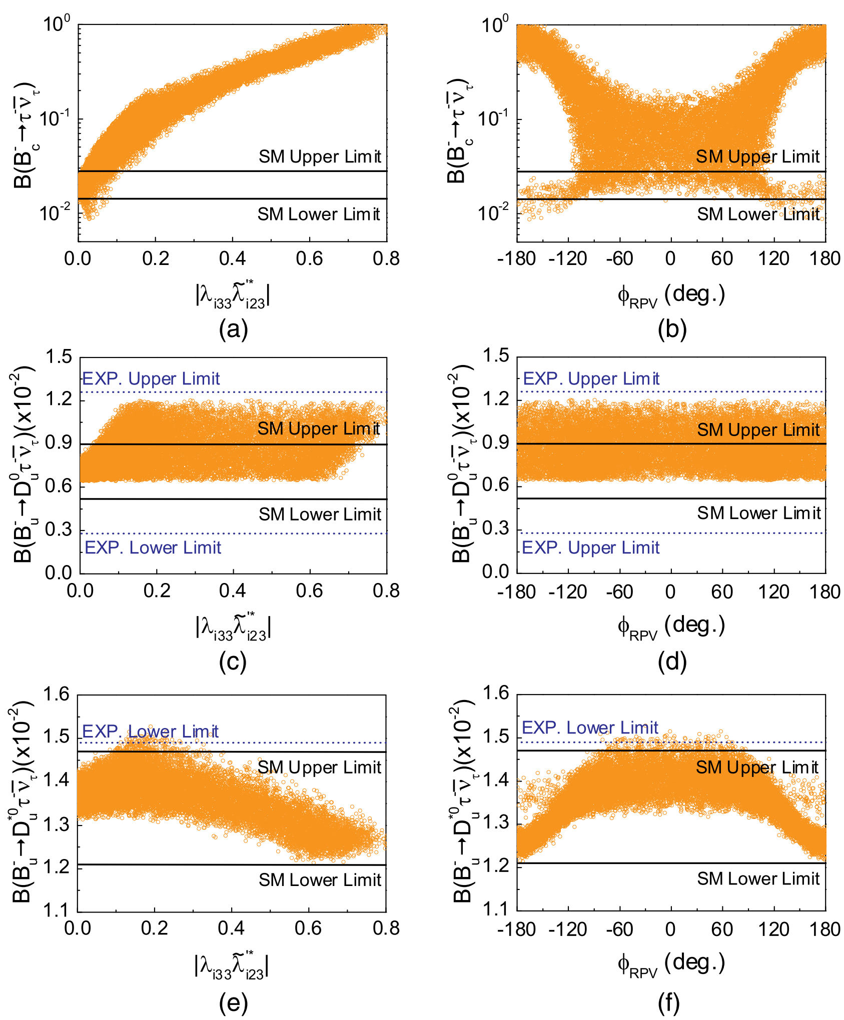

FIG. 4. Constrained effects of the slepton exchange coupling $\lambda_{i33}\tilde{\lambda}'^{*}_{i23}$ in the exclusive $b \to c\tau^-\bar{\nu}_\tau$ decays.

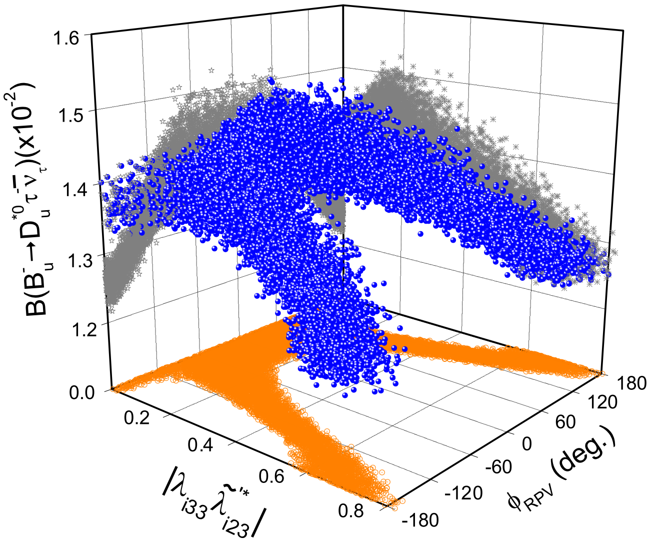

FIG. 5. The $\lambda_{i33}\tilde{\lambda}'^*_{i23}$ coupling effects on $\mathcal{B}(B_u^- \to D^{*0}\tau^-\bar{\nu}_\tau)$. This plot shows the change trends of $\mathcal{B}(B_u^- \to D^{*0}\tau^-\bar{\nu}_\tau)$ with $|\lambda_{i33}\tilde{\lambda}'^*_{i23}|$ and its weak phase $\phi_{\rm RPV}$ with blue little balls. We also give projections on three perpendicular planes. The $|\lambda_{i33}\tilde{\lambda}'^*_{i23}| - \phi_{\rm RPV}$ plane displays the allowed regions of $\lambda_{i33}\tilde{\lambda}'^*_{i23}$, which is the same as Fig. 3. The $\mathcal{B}(B_u^- \to D^{*0}\tau^-\bar{\nu}_\tau) - |\lambda_{i33}\tilde{\lambda}'^*_{i23}|$ plane displays the sensitivity of $\mathcal{B}(B_u^- \to D^{*0}\tau^-\bar{\nu}_\tau)$ to $|\lambda_{i33}\tilde{\lambda}'^*_{i23}|$, which is the same as Fig. 4(e), and the $\mathcal{B}(B_u^- \to D^{*0}\tau^-\bar{\nu}_\tau) - \phi_{\rm RPV}$ is the same as Fig. 4(f).

phase $\phi_{\rm RPV}$ are not independent of each other, and the three-dimensional scatter plots shown in Fig. 5 are more suitable ways to display the dependence. From Fig. 5, we can see that when $|\lambda_{i33}\tilde{\lambda}'^*_{i23}| \in [0.11, 0.35]$ and its phase $\phi_{\rm RPV} \in [-83°, 71°]$ at the same time, $\mathcal{B}(B_u^- \to D_u^{*0}\tau^-\bar{\nu}_\tau)$ could be equal or greater than its lower limits of the present 95% C.L. experimental average.

In Fig. 6(a), we show another RPV prediction with the green "–" labeled as "SM + RPVII", which is constrained by all the above mentioned 95% C.L. experimental measurements except $\mathcal{R}(D)$. We can see that the constrained $\lambda_{i33}\tilde{\lambda}'^*_{i23}$ couplings have very large effects on $d\mathcal{B}(B_u^- \to D_u^0\tau^-\bar{\nu}_\tau)/ds$ at whole s regions, and the 95% C.L. experimental bound of $\mathcal{R}(D)$ gives quite obvious constraints at middle and high s regions. Figure 6(b) shows us that the constrained $\lambda_{i33}\tilde{\lambda}'^*_{i23}$ couplings have some effects on $d\mathcal{B}(B_u^- \to D_u^{*0}\tau^-\bar{\nu}_\tau)/ds$ at the middle s region. As displayed in Figs. 6(c) and 6(d), the constrained $\lambda_{i33}\tilde{\lambda}'^*_{i23}$ couplings have significant effects on $\bar{\mathcal{A}}_{\rm FB}(B_u^- \to D_u^{(*)0}\tau^-\bar{\nu}_\tau)$ at the whole s region.

D. Ratios $\mathcal{R}(D)$ and $\mathcal{R}(D^*)$

For the exclusive $b \to c\ell^-\bar{\nu}_\ell$ decays, the ratios of the branching ratios have been accurately measured by LHCb, *BABAR*, and Belle [3,4,7,8] Collaborations. At the 95% C.L., their experimental averaged ranges, SM predictions, and RPV SUSY predictions are listed in Table IV. We can see that $\mathcal{R}(D)$ is constrained by its 95% C.L.

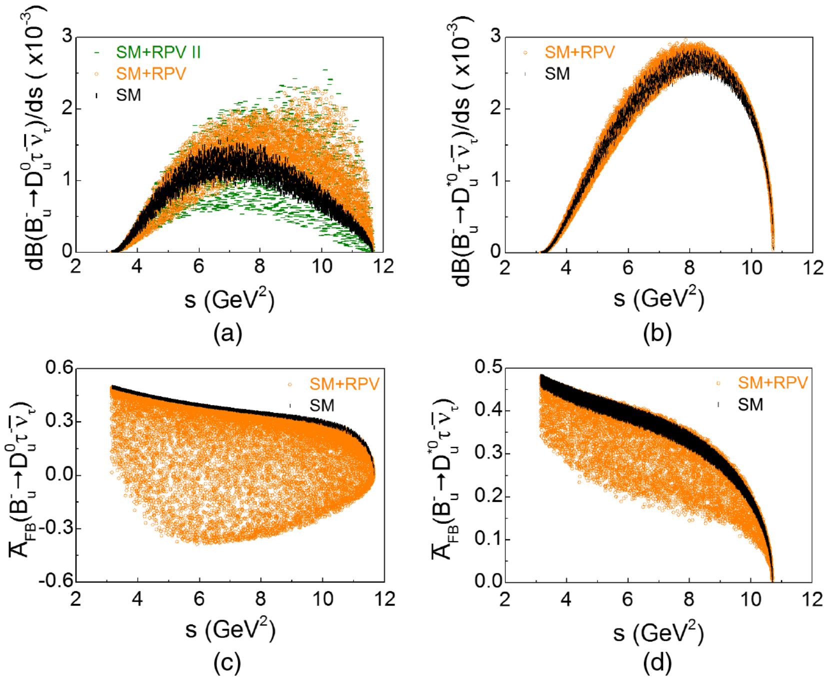

FIG. 6. Constrained slepton exchange effects on the differential branching ratios and the normalized FB asymmetries of $B_u^- \to D_u^{(*)0}\tau^-\bar{\nu}_\tau$ decays.

TABLE IV. Ratios $\mathcal{R}(D)$ and $\mathcal{R}(D^*)$ in the exclusive $b \to c\ell^-\bar{\nu}_\ell$ decays.

Observable	Exp. data	SM predictions	SUSY/$\lambda_{i33}\tilde{\lambda}'^*_{i23}$
$\mathcal{R}(D)$	[0.294, 0.488]	[0.251, 0.343]	[0.294, 0.488]
$\mathcal{R}(D^*)$	[0.280, 0.364]	[0.242, 0.263]	[0.226, 0.278]

experimental measurements. As for $\mathcal{R}(D^*)$, the maximum of the RPV prediction almost reaches the lower limit of its 95% C.L. experimental measurements.

In order to compare easily, we display the 95% C.L. SM predictions, 95% C.L. RPV SUSY predictions, 95% C.L. experimental measurements from *BABAR* as well as Belle, and their experimental average from the Heavy Flavor Averaging Group [9] listed in Eq. (1) within 5σ on the $\mathcal{R}(D) - \mathcal{R}(D^*)$ plane in Fig. 7, and we can clearly see that our RPV SUSY predictions have about 2σ deviations from the experimental averaged values on the $\mathcal{R}(D) - \mathcal{R}(D^*)$ plane. At the 95% C.L., the RPV SUSY predictions of $\mathcal{R}(D)$ and $\mathcal{R}(D^*)$ are consistent with each experimental measurement from *BABAR* and Belle. Note that since LHCb only reported the measurement of $R(D^*)$ but not $\mathcal{R}(D)$, we do not display the measurement of $R(D^*)$ from LHCb in Fig. 7, nevertheless, at the 95% C.L., $R(D^*) \in [0.257, 0.415]$ from LHCb also agrees with our RPV SUSY prediction. The error of the experiential average is much smaller than each one of the measurements from *BABAR*, Belle, and LHCb Collaborations, at the 99% C.L., and the RPV SUSY predictions for $\mathcal{R}(D)$ and $\mathcal{R}(D^*)$ agree with the experimental averages.

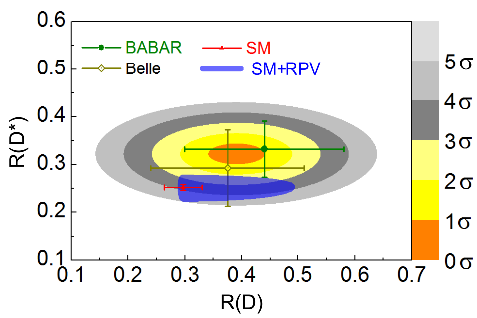

FIG. 7. Ratios $\mathcal{R}(D)$ and $\mathcal{R}(D^*)$. The theoretical predictions and experimental measurements from *BABAR* and Belle are shown at the 95% C.L., and the experiential average from the Heavy Flavor Averaging Group [9], which are listed in Eq. (1), are given within 5σ. Noted that, since LHCb only reported the measurement of $R(D^*)$ but not $\mathcal{R}(D)$, we do not display the measurement from LHCb in this plot.

Now, we give the sensitivities of $\mathcal{R}(D^{(*)})$ to the slepton exchange couplings. We plot $\mathcal{R}(D)$ and $\mathcal{R}(D^*)$ as functions of the moduli and weak phases of $\lambda_{i11}\tilde{\lambda}'^*_{i23}$, $\lambda_{i22}\tilde{\lambda}'^*_{i23}$, and $\lambda_{i33}\tilde{\lambda}'^*_{i23}$, and we found that ratios $\mathcal{R}(D)$ and $\mathcal{R}(D^*)$ are not sensitive to $\lambda_{i11}\tilde{\lambda}'^*_{i23}$ and $\lambda_{i22}\tilde{\lambda}'^*_{i23}$ couplings. Therefore, we only show the sensitivities to the moduli and weak phases of $\lambda_{i33}\tilde{\lambda}'^*_{i23}$ couplings in Fig. 8. As displayed in Figs. 8(a) and 8(b), the SUSY prediction with $\lambda_{i33}\tilde{\lambda}'^*_{i23}$ couplings exactly match the experimental upper and lower limits since the experimental average of $\mathcal{R}(D)$ at the 95% C.L. gives a strong bound on this SUSY prediction. Moreover, we can see that $\mathcal{R}(D)$ is sensitive to the $|\lambda_{i33}\tilde{\lambda}'^*_{i23}|$

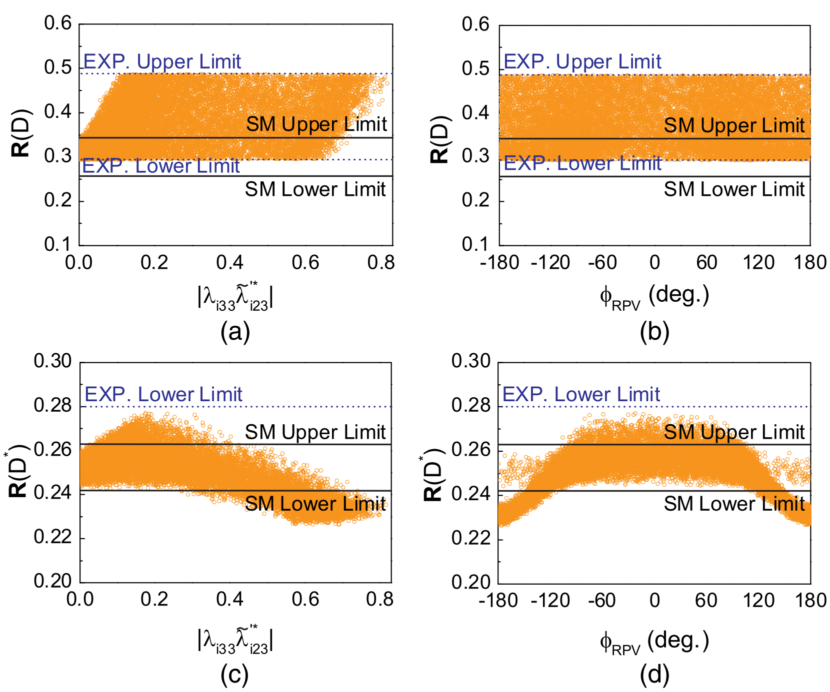

FIG. 8. Constrained effects of RPV coupling $\lambda_{i33}\tilde{\lambda}'^*_{i23}$ due to the slepton exchange in ratios $\mathcal{R}(D^{(*)})$.

coupling, and the experimental bound of $\mathcal{R}(D)$ gives obvious constraints on $|\lambda_{i33}\tilde{\lambda}'^{*}_{i23}|$. In Figs. 8(c) and 8(d), $\mathcal{R}(D^*)$ is very sensitive to both the moduli and weak phases of the $\lambda_{i33}\tilde{\lambda}'^{*}_{i23}$ couplings, and it could have a maximum at $|\lambda_{i33}\tilde{\lambda}'^{*}_{i23}| \in [0.11, 0.35]$ and $\phi_{\rm RPV} \in [-83°, 71°]$.

IV. CONCLUSION

Motivated by the recent experimental data of ratios $\mathcal{R}(D^{(*)})$ reported by LHCb, *BABAR*, and Belle Collaborations, we have studied the RPV SUSY effects in the leptonic and semileptonic decays, $B_c^- \to \ell^-\bar{\nu}_\ell$, $B_u^- \to D_u^0\ell^-\bar{\nu}_\ell$, $B_u^- \to D_u^{*0}\ell^-\bar{\nu}_\ell$, $B_d^0 \to D_d^+\ell^-\bar{\nu}_\ell$, and $B_d^0 \to D_d^{*+}\ell^-\bar{\nu}_\ell$. Considering the theoretical uncertainties and the experimental errors at the 95% C.L., we have constrained the parameter spaces of relevant RPV couplings from the present experimental data. We have found that the effects of the squark exchange couplings could be neglected in the exclusive $b \to c\ell^-\bar{\nu}_\ell$ decays. As for the slepton exchange couplings, the strongest bounds on $\lambda_{i11}\tilde{\lambda}'^{*}_{i23}$ and $\lambda_{i22}\tilde{\lambda}'^{*}_{i23}$ came from the exclusive $b \to s\ell^+\ell^-$ decays, and the bounds on $\lambda_{i33}\tilde{\lambda}'^{*}_{i23}$ have been obtained from the exclusive $b \to c\ell^-\bar{\nu}_\ell$ decays for the first time.

Furthermore, we have predicted the constrained slepton exchange effects on the branching ratios, differential branching ratios, normalized FB asymmetries of the charged leptons, and ratios of the semilepton decay branching ratios. We have found that $\mathcal{B}(B_c^- \to \ell^-\bar{\nu}_\ell)$ and $\mathcal{B}(B \to D^*\tau^-\bar{\nu}_\tau)$ are very sensitive to the constrained slepton exchange couplings, and the constrained slepton exchange couplings have great effects on $d\mathcal{B}(B \to D\tau^-\bar{\nu}_\tau)/ds$, $\bar{\mathcal{A}}_{\rm FB}(B \to De^-\bar{\nu}_e)$, $\bar{\mathcal{A}}_{\rm FB}(B \to D\tau^-\bar{\nu}_\tau)$, and $\bar{\mathcal{A}}_{\rm FB}(B \to D^*\tau^-\bar{\nu}_\tau)$; in addition, the sign of $\bar{\mathcal{A}}_{\rm FB}(B \to De^-\bar{\nu}_e)$ could be changed by the large slepton exchange couplings $\lambda_{i11}\tilde{\lambda}'^{*}_{i23}$.

For $\mathcal{R}(D)$ and $\mathcal{R}(D^*)$, they are very sensitive to the constrained $\lambda_{i33}\tilde{\lambda}'^{*}_{i23}$ couplings but not sensitive to the constrained $\lambda_{i11}\tilde{\lambda}'^{*}_{i23}$ and $\lambda_{i22}\tilde{\lambda}'^{*}_{i23}$ couplings from the exclusive $b \to s\ell^+\ell^-$ decays. The constrained $\lambda_{i33}\tilde{\lambda}'^{*}_{i23}$ couplings could enhance $\mathcal{R}(D)$ to its 95% C.L. experimental range. Although the constrained $\lambda_{i33}\tilde{\lambda}'^{*}_{i23}$ couplings may enhance $\mathcal{R}(D^*)$, its maximum still has a 2σ deviation from the 95% C.L. experimental average. Nevertheless, the constrained slepton exchange couplings could let $\mathcal{R}(D^*)$ reach each 95% C.L. experimental range from *BABAR*, Belle, and LHCb Collaborations. In addition, at the 99% C.L., the RPV prediction for $\mathcal{R}(D^*)$ agrees with the experimental averages.

With the running LHCb and the forthcoming Belle-II experiments, heavy flavor physics is entering a precision era, which would present new features to examine various NP models, including the RPV SUSY model studied in this paper. Our results could be useful for probing the RPV SUSY effects and will correlate strongly with searches for the direct RPV SUSY signals in future experiments.

ACKNOWLEDGMENTS

The work of Ru-Min Wang was supported by Program for New Century Excellent Talents in University (Grant No. NCET-12-0698). The works of Yuan-Guo Xu, Ying-Ying Fan, and Qin Chang were supported by the National Natural Science Foundation of China (Grants No. U1204113, No. 11505148, and No. 11475055).

[1] N. E. Adam *et al.* (CLEO Collaboration), Phys. Rev. D **67**, 032001 (2003).
[2] W. Dungel *et al.* (Belle Collaboration), Phys. Rev. D **82**, 112007 (2010).
[3] M. Huschle *et al.* (Belle Collaboration), Phys. Rev. D **92**, 072014 (2015).
[4] J. P. Lees *et al.* (*BABAR* Collaboration), Phys. Rev. Lett. **109**, 101802 (2012).
[5] B. Aubert *et al.* (*BABAR* Collaboration), Phys. Rev. D **77**, 032002 (2008).
[6] B. Aubert *et al.* (*BABAR* Collaboration), Phys. Rev. D **79**, 012002 (2009).
[7] J. P. Lees *et al.* (*BABAR* Collaboration), Phys. Rev. D **88**, 072012 (2013).
[8] R. Aaij *et al.* (LHCb Collaboration), Phys. Rev. Lett. **115**, 111803 (2015).
[9] Y. Amhis *et al.* (Heavy Flavor Averaging Group Collaboration), arXiv:1412.7515.
[10] S. Fajfer, J. F. Kamenik, and I. Nisandzic, Phys. Rev. D **85**, 094025 (2012).
[11] J. F. Kamenik and F. Mescia, Phys. Rev. D **78**, 014003 (2008).
[12] L. Calibbi, A. Crivellin, and T. Ota, Phys. Rev. Lett. **115**, 181801 (2015).
[13] A. Crivellin, J. Heeck, and P. Stoffer, Phys. Rev. Lett. **116**, 081801 (2016).
[14] S. Bhattacharya, S. Nandi, and S. K. Patra, Phys. Rev. D **93**, 034011 (2016).
[15] J. A. Bailey *et al.*, Phys. Rev. D **92**, 034506 (2015).
[16] H. Na, C. M. Bouchard, G. P. Lepage, C. Monahan, and J. Shigemitsu, Phys. Rev. D **92**, 054510 (2015).
[17] J. A. Bailey *et al.*, Phys. Rev. Lett. **109**, 071802 (2012).
[18] J. A. Bailey *et al.*, Phys. Rev. D **85**, 114502 (2012); **86**, 039904(E) (2012).
[19] R. N. Faustov and V. O. Galkin, Mod. Phys. Lett. A **27**, 1250183 (2012).

[20] S. Fajfer, J. F. Kamenik, I. Nisandzic, and J. Zupan, Phys. Rev. Lett. **109**, 161801 (2012).
[21] A. Datta, M. Duraisamy, and D. Ghosh, Phys. Rev. D **86**, 034027 (2012).
[22] D. Choudhury, D. K. Ghosh, and A. Kundu, Phys. Rev. D **86**, 114037 (2012).
[23] B. Bhattacharya, A. Datta, D. London, and S. Shivashankara, Phys. Lett. B **742**, 370 (2015).
[24] M. Duraisamy, P. Sharma, and A. Datta, Phys. Rev. D **90**, 074013 (2014).
[25] M. Duraisamy and A. Datta, J. High Energy Phys. 09 (2013) 059.
[26] D. Becirevic, N. Kosnik, and A. Tayduganov, Phys. Lett. B **716**, 208 (2012).
[27] X. G. He and G. Valencia, Phys. Rev. D **87**, 014014 (2013).
[28] S. Fajfer and I. Nisandzic, *Proceedings of CKM 2012, 7th International Workshop on the CKM Unitarity Triangle, University of Cincinnati, USA, 2012*, arXiv:1301.1167.
[29] A. Pich, Nucl. Phys. B, Proc. Suppl. **253–255**, 193 (2014).
[30] G. Ricciardi, *Proc. Sci.*, ConfinementX2014 (2014) 145, arXiv:1301.4389.
[31] Y. Y. Fan, W. F. Wang, S. Cheng, and Z. J. Xiao, Chin. Sci. Bull. **59**, 125 (2014).
[32] Z. J. Xiao, Y. Y. Fan, W. F. Wang, and S. Cheng, Chin. Sci. Bull. **59**, 3787 (2014).
[33] Y. Y. Fan, Z. J. Xiao, R. M. Wang, and B. Z. Li, Sci. Bull. **60**, 2009 (2015).
[34] S. Stone, *Proc. Sci.*, ICHEP2012 (2013) 033, arXiv: 1212.6374.
[35] Y. Sakaki and H. Tanaka, Phys. Rev. D **87**, 054002 (2013).
[36] A. Crivellin, C. Greub, and A. Kokulu, Phys. Rev. D **86**, 054014 (2012).
[37] A. Celis, M. Jung, X. Q. Li, and A. Pich, J. Phys. Conf. Ser. **447**, 012058 (2013).
[38] A. Celis, M. Jung, X. Q. Li, and A. Pich, J. High Energy Phys. 01 (2013) 054.
[39] D. Becirevic, S. Fajfer, I. Nisandzic, and A. Tayduganov, arXiv:1602.03030.
[40] C. S. Aulakh and R. N. Mohapatra, Phys. Lett. B **119**, 136 (1982); L. J. Hall and M. Suzuki, Nucl. Phys. **B231**, 419 (1984); S. Dawson, Nucl. Phys. **B261**, 297 (1985).
[41] G. G. Ross and J. W. F. Valle, Phys. Lett. **151B**, 375 (1985); J. R. Ellis, G. Gelmini, C. Jarlskog, G. G. Ross, and J. W. F. Valle, Phys. Lett. **150B**, 142 (1985).
[42] C. S. Kim and R. M. Wang, Phys. Rev. D **77**, 094006 (2008).
[43] A. Celis, arXiv:1410.1858.
[44] M. Chemtob, Prog. Part. Nucl. Phys. **54**, 71 (2005).
[45] S. Nandi and J. P. Saha, Phys. Rev. D **74**, 095007 (2006).
[46] Y. G. Xu, R. M. Wang, and Y. D. Yang, Phys. Rev. D **74**, 114019 (2006).
[47] C. S. Kim and R. M. Wang, Phys. Lett. B **681**, 44 (2009).
[48] R. M. Wang, Y. G. Xu, M. L. Liu, and B. Z. Li, J. High Energy Phys. 12 (2010) 034.
[49] R. M. Wang, Y. G. Xu, Y. L. Wang, and Y. D. Yang, Phys. Rev. D **85**, 094004 (2012).
[50] C. Li, C. D. Lu, and X. D. Gao, Commun. Theor. Phys. **59**, 711 (2013).
[51] H. K. Dreiner, K. Nickel, and F. Staub, Phys. Rev. D **88**, 115001 (2013).
[52] A. K. Alok and S. K. Gupta, Eur. Phys. J. C **65**, 491 (2010).
[53] B. Colquhoun, C. T. H. Davies, J. Kettle, J. Koponen, A. T. Lytle, R. J. Dowdall, and G. P. Lepage (HPQCD Collaboration), Phys. Rev. D **91**, 114509 (2015).
[54] K. A. Olive *et al.* (Particle Data Group Collaboration), Chin. Phys. C **38**, 090001 (2014).